Eurographics Symposium on Geometry Processing (2006)
Konrad Polthier, Alla Sheffer (Editors)

Spherical Barycentric Coordinates

Torsten Langer, Alexander Belyaev, Hans-Peter Seidel

MPI Informatik

Abstract

We develop spherical barycentric coordinates. Analogous to classical, planar barycentric coordinates that describe the positions of points in a plane with respect to the vertices of a given planar polygon, spherical barycentric coordinates describe the positions of points on a sphere with respect to the vertices of a given spherical polygon. In particular, we introduce spherical mean value coordinates that inherit many good properties of their planar counterparts. Furthermore, we present a construction that gives a simple and intuitive geometric interpretation for classical barycentric coordinates, like Wachspress coordinates, mean value coordinates, and discrete harmonic coordinates.

One of the most interesting consequences is the possibility to construct mean value coordinates for arbitrary polygonal meshes. So far, this was only possible for triangular meshes. Furthermore, spherical barycentric coordinates can be used for all applications where only planar barycentric coordinates were available up to now. They include Bézier surfaces, parameterization, free-form deformations, and interpolation of rotations.

Categories and Subject Descriptors (according to ACM CCS): I.3.5 [Computer Graphics]: Computational Geometry and Object Modeling

1. Introduction

Barycentric coordinates are a special kind of local coordinates that express the location of a point with respect to a given triangle. They were developed by Möbius [Möb27] in the nineteenth century. Wachspress extended the notion of barycentric coordinates to arbitrary convex polygons [Wac75]; another approach is due to Sibson [Sib80]. In recent years, the research on barycentric coordinates has been intensified and led to a general theory of barycentric coordinates and extensions to higher dimensions [FHK06, FKR05, JSWD05, JSW05, JW05]. Barycentric coordinates are natural coordinates for meshes and have many applications including parameterization [DMA02, SAPH04], free-form deformations [SP86, JSW05], finite elements [AO06, SM06], shading [Gou71, Pho75], and elementary geometry.

Our main contribution is the extension of the notion of barycentric coordinates in several directions as follows:

- We introduce spherical barycentric coordinates. They are analogues of the classical barycentric coordinates, but they are defined for polygons on a sphere instead of a plane.
- We construct three-dimensional barycentric coordinates for arbitrary, closed polygonal meshes.
- We show that the vector coordinates in [JSWD05] and the 3D mean value coordinates for triangular meshes in [FKR05, JSW05] are special cases of our constructions.

The extension to polygonal meshes is an important generalization as noted in [JSW05]. In particular, it makes it possible to use barycentric coordinates in conjunction with subdivision surfaces and the recently introduced conical meshes [LPW*06].

Let $P = (\mathbf{v}_j)_{j=1..n}$ be a polygon with vertices $\mathbf{v}_j$. *Barycentric coordinates* $\lambda_i(\mathbf{v};P) = \lambda_i\left(\mathbf{v};(\mathbf{v}_j)_{j=1..n}\right)$ of a point $\mathbf{v}$ are continuous functions that satisfy the following properties (2) and (3) for all points $\mathbf{v}$ inside the polygon. If property (1) is additionally fulfilled for all convex polygons, we call them *positive barycentric coordinates*.

$$\forall i\ \lambda_i(\mathbf{v};P) > 0 \qquad \text{positivity,} \qquad (1)$$

$$\sum_i \lambda_i(\mathbf{v};P) = 1 \qquad \text{partition of unity,} \qquad (2)$$

$$\sum_i \lambda_i(\mathbf{v};P)\mathbf{v}_i = \mathbf{v} \qquad \text{linear precision.} \qquad (3)$$

If P is a triangle, its barycentric coordinates are uniquely determined by these conditions. In general, it is only possible to fulfill all three properties for convex polygons. We use also λ_i or $\lambda_i(\mathbf{v})$ if P and the point $\mathbf{v}$ are clear from the context. If a partition of unity (2) is not given, we speak of *homogeneous coordinates*. They can be normalized to satisfy property (2) if and only if $\sum_i \lambda_i(\mathbf{v}) \neq 0$. Property (3) is called "linear precision" since it ensures the correct interpolation of all linear functions f:

$$\sum_i \lambda_i(\mathbf{v}) f(\mathbf{v}_i) = f(\mathbf{v}). \tag{4}$$

The construction of barycentric coordinates for polygons with more than three vertices had been an open problem for a long time. The coordinates introduced by Wachspress [Wac75] are defined for arbitrary convex polygons $P \subset \mathbb{R}^2$ and satisfy properties (1)–(3), but they are in general only defined inside of convex polygons. This restriction was overcome with the introduction of the mean value coordinates by Floater [Flo03]. They are defined in the whole plane for convex and non-convex polygons and can even be extended to multiple polygons [HF06]. In [FHK06], an overview over all similarity invariant, homogeneous coordinates is given. In particular, it is shown that Wachspress coordinates and mean value coordinates are the only similarity invariant, positive barycentric three-point coordinates. Recently, Wachspress coordinates and mean value coordinates were generalized to polytopes of higher dimensions. However, this was only possible for convex polytopes (3D Wachspress coordinates) [War96, JSWD05] and for polytopes with simplicial boundary (3D mean value coordinates) [FKR05, JSW05].

Spherical barycentric coordinates constitute another variant of barycentric coordinates. They have been studied first by Möbius [Möb46] and were introduced to computer graphics by Alfeld et al. [ANS96]. Spherical barycentric coordinates express the location of a point $\mathbf{v}$ on a sphere with respect to the vertices $\mathbf{v}_i$ of a given spherical triangle P. Since partition of unity (2) and linear precision (3) contradict each other on spheres, Alfeld et al. chose to relax the former condition to

$$\sum_i \lambda_i \geq 1. \tag{2'}$$

Ju et al. [JSWD05] extended spherical barycentric coordinates (they called them "vector coordinates") from spherical triangles to arbitrary convex, spherical polygons. However, non-convex spherical polygons still posed a problem.

In this paper, we show how arbitrary barycentric coordinates from the family of planar barycentric coordinates [FHK06] can be defined on a sphere (Section 2.1). In particular, we introduce spherical mean value coordinates that inherit many good properties of their planar counterparts and are defined for arbitrary spherical polygons (Section 2.2). We show that the vector coordinates by Ju et al. [JSWD05] coincide with spherical Wachspress coordinates from our family (Section 2.3). Furthermore, we show how 3D barycentric coordinates (in particular, mean value coordinates) for arbitrary polygonal meshes can be defined with the help of our spherical mean value coordinates (Section 3). Finally, we discuss several applications including space deformations and Bézier surfaces (Section 4). In addition, we provide a novel, geometric interpretation of planar barycentric coordinates (Appendix A).

2. Spherical barycentric coordinates

In this section, we deal with the problem of finding (positive) coefficients λ_i for vectors $\mathbf{v}_i \in \mathbb{R}^3$ such that their linear combination is $\mathbf{v} \in \mathbb{R}^3$. If we restrict ourselves to vectors of unit length, the λ_i represent barycentric coordinates for $\mathbf{v}$ with respect to the $\mathbf{v}_i$ on the unit sphere. First, we give a general introduction. Then, we develop spherical mean value coordinates (Equation (8)) and spherical Wachspress coordinates (Section 2.3).

While Equations (1)–(3) are well-chosen to characterize planar barycentric coordinates, it is obviously not possible to fulfill all three conditions if the vertices $\mathbf{v}_i$ and the point $\mathbf{v}$ are located on a sphere instead of a plane. This is especially easy to see if P is a triangle with three vertices. In particular, Equations (2) and (3) contradict each other since the former condition requires all points described by $\sum_i \lambda_i \mathbf{v}_i$ to lie in the triangle plane while the latter condition demands that this sum yields a point $\mathbf{v}$ that lies not in this plane but on the sphere. A similar observation was made in [BW92].

Consequently, we have to relax the above conditions. We follow the suggestion in [ANS96] and replace Equation (2) by (2′). Of course, by dividing by $\sum_j \lambda_j$, we could also obtain coordinates that constitute a partition of unity (2) instead of satisfying the linear precision property (3) if desired. However, for our applications, in particular for constructing barycentric coordinates for meshes, linear precision is more important. Note that this property still implies that linear functions *defined on* $\mathbb{R}^3$ are correctly interpolated (Equation (4)). Constant functions, however, cannot be correctly interpolated if a partition of unity (2) is not given. A different approach that preserves the partition of unity was proposed in [BF01]. We call a set of coordinates λ_i satisfying conditions (2′) and (3) *spherical barycentric coordinates*. If P is a triangle, then there exists obviously a unique solution: the unique linear combination of the vectors $\mathbf{v}_1$, $\mathbf{v}_2$, and $\mathbf{v}_3$ such that $\sum_{i=1}^{3} \lambda_i \mathbf{v}_i = \mathbf{v}$. A geometric interpretation of these spherical barycentric coordinates was given in [ANS96].

2.1. Definition of spherical barycentric coordinates

In this section, we show how barycentric coordinates can be defined for arbitrary polygons on a sphere.

Definition 2.1 A *spherical polygon P* consists of a set of distinct vertices $\mathbf{v}_i$ located on a sphere and a set of edges $(\mathbf{v}_i, \mathbf{v}_{i+1})$ that connect the vertices $\mathbf{v}_i$ and $\mathbf{v}_{i+1}$ by geodesic lines (these are the arcs of great circles on the sphere).

We consider a spherical polygon on the unit sphere centered at the origin. Let $\mathbf{v}$ be a point on the sphere. Let $\widehat{\mathbf{v}_i}$ be

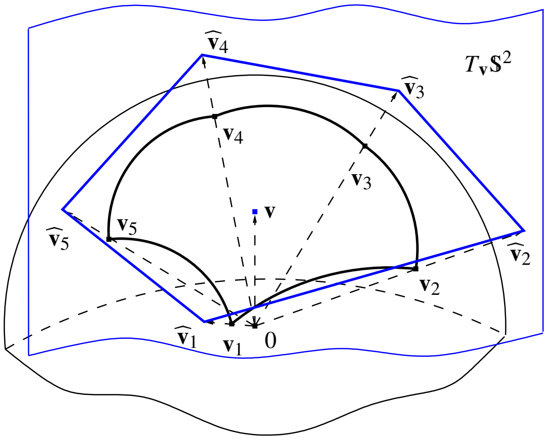

Figure 1: *Construction of spherical barycentric coordinates.*

the intersection points of the line given by $\mathbf{v}_i$ and the tangent plane $T_{\mathbf{v}}\mathbb{S}^2$ at $\mathbf{v}$ to the sphere (see Figures 1 and 2). The points $\widehat{\mathbf{v}}_i$ determine a polygon $\widehat{P}$ (shown in blue) in the plane $T_{\mathbf{v}}\mathbb{S}^2$. (The map $\mathbf{v}_i \mapsto \widehat{\mathbf{v}}_i$ is a gnomonic projection. It is especially useful for our purpose since it projects geodesics to straight lines.) Now, we can compute the planar barycentric coordinates $\widehat{\lambda}_i$ of $\mathbf{v}$ with respect to $\widehat{P}$. The 3D position of $\mathbf{v}$ is an affine linear function on $T_{\mathbf{v}}\mathbb{S}^2$. Consequently, any set $\widehat{\lambda}_i$ of planar barycentric coordinates yields, by Equations (2) and (3),

$$\sum_i \widehat{\lambda}_i \widehat{\mathbf{v}}_i = \mathbf{v}.$$

To obtain spherical barycentric coordinates λ_i of $\mathbf{v}$ that satisfy the linear precision property (3), we define them by

$$\sum_i \lambda_i \mathbf{v}_i = \mathbf{v}, \qquad \lambda_i := \langle \mathbf{v}_i, \widehat{\mathbf{v}}_i \rangle \widehat{\lambda}_i \tag{5}$$

where $\langle \cdot, \cdot \rangle$ denotes the usual scalar product in $\mathbb{R}^3$. Note that $\langle \mathbf{v}_i, \widehat{\mathbf{v}}_i \rangle$ is just $\pm \|\widehat{\mathbf{v}}_i\|$. Although this value becomes very large and finally undefined if the angle θ_i between $\mathbf{v}$ and $\mathbf{v}_i$ approaches $\frac{\pi}{2}$, this is usually compensated by a shrinkage of $\widehat{\lambda}_i$ such that the definition of λ_i can be extended continuously to the case $\theta_i = \frac{\pi}{2}$. We demonstrate this in Sections 2.2 and 2.3 for spherical mean value and spherical Wachspress coordinates. Note that basically the same construction can be used to obtain planar barycentric coordinates from spherical barycentric coordinates. It follows that there is a bijection between planar barycentric coordinates and spherical barycentric coordinates.

Finally, we remark that these coordinates can also be extended to vectors $\mathbf{v}_i$ and $\mathbf{v}$ of arbitrary length by defining

$$\lambda_i\Big(\mathbf{v}; (\mathbf{v}_j)_{j=1..n}\Big) := \frac{\|\mathbf{v}\|}{\|\mathbf{v}_i\|} \cdot \lambda_i\Big(\tfrac{\mathbf{v}}{\|\mathbf{v}\|}; (\tfrac{\mathbf{v}_j}{\|\mathbf{v}_j\|})_{j=1..n}\Big). \tag{6}$$

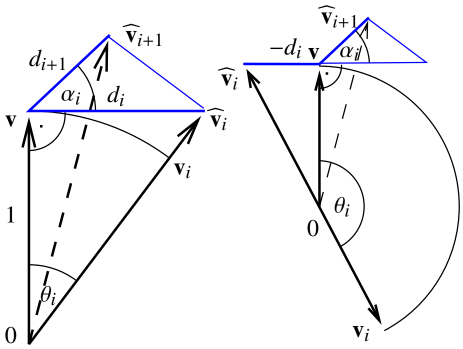

Figure 2: *Notation for spherical barycentric coordinates.*

2.2. Spherical mean value coordinates

We now develop spherical mean value coordinates. They inherit positivity from their planar counterparts: the $\lambda_i(\mathbf{v})$ are positive if $\mathbf{v}$ is contained in the kernel of the polygon given by the $\mathbf{v}_i$. If $\mathbf{v}$ is contained in the convex hull of the $\mathbf{v}_i$, this can always be arranged by reordering the vertices $\mathbf{v}_i$ with respect to their polar angle around $\mathbf{v}$. (The kernel is the region inside the polygon from which the whole polygon is "visible".)

Planar mean value coordinates are given by Floater's formula [Flo03]

$$\widehat{\lambda}_i = \frac{w_i}{\sum_j w_j}, \qquad w_i = \frac{\tan\frac{\alpha_{i-1}}{2} + \tan\frac{\alpha_i}{2}}{d_i} \tag{7}$$

where α_i is the signed angle between $\widehat{\mathbf{v}}_i - \mathbf{v}$ and $\widehat{\mathbf{v}}_{i+1} - \mathbf{v}$ and d_i is the distance $\|\widehat{\mathbf{v}}_i - \mathbf{v}\|$. As shown in Figure 2, α_i is given by the dihedral, signed angle between the planes determined by $\mathbf{v}$, $\mathbf{v}_i$, and the origin, and $\mathbf{v}$, $\mathbf{v}_{i+1}$, and the origin, respectively. That is, α_i is the signed angle between $\mathbf{v} \times \mathbf{v}_i$ and $\mathbf{v} \times \mathbf{v}_{i+1}$. The distance d_i is given by $d_i = \tan\theta_i$ where θ_i is the angle between $\mathbf{v}$ and $\mathbf{v}_i$. By inserting these terms into Equations (7) and (5) and using $\langle \mathbf{v}_i, \widehat{\mathbf{v}}_i \rangle = \frac{1}{\cos\theta_i}$, we obtain

$$\lambda_i(\mathbf{v}) = \frac{\tan\frac{\alpha_{i-1}}{2} + \tan\frac{\alpha_i}{2}}{\sin\theta_i} \Bigg/ \sum_j \cot\theta_j \Big(\tan\frac{\alpha_{j-1}}{2} + \tan\frac{\alpha_j}{2}\Big). \tag{8}$$

This formula gives us a continuous definition of λ_i for arbitrary $\mathbf{v}$. But for a $\mathbf{v}$ with $\theta_i > \frac{\pi}{2}$, it implies that in the projected polygon $\widehat{P}$, the vector $\widehat{\mathbf{v}}_i - \mathbf{v}$ has negative length (and is still oriented like $\mathbf{v} - \widehat{\mathbf{v}}_i$; this is the reason that α_i is measured as the angle between $-(\widehat{\mathbf{v}}_i - \mathbf{v})$ and $\widehat{\mathbf{v}}_{i+1} - \mathbf{v}$ instead of $\widehat{\mathbf{v}}_i - \mathbf{v}$ and $\widehat{\mathbf{v}}_{i+1} - \mathbf{v}$), as indicated on the right of Figure 2. It can be seen that the planar mean value coordinates still satisfy linear precision (3) for this case (for example, this is implied by the construction in Appendix A). Therefore, the derived spherical barycentric coordinates fulfill linear precision as well.

From Equation (8), it is easy to see that the spherical mean value coordinates are well-defined and positive if $\mathbf{v}$ is inside

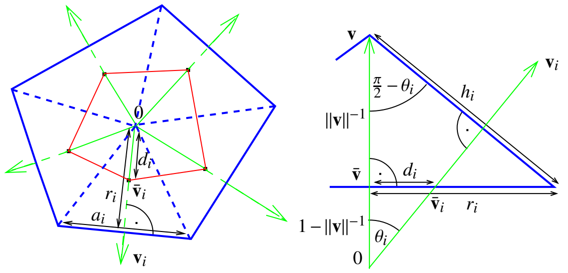

Figure 3: *Bottom and side view of the polar dual.*

a convex spherical polygon and $\theta_i < \frac{\pi}{2}$ for all θ_i. For such polygons, inequality (2′) is implied by the triangle inequality.

2.3. Relation to Ju et al.'s vector coordinates

In this section, we show that the coordinates that were introduced by Ju et al. [JSWD05] to express a vector $\mathbf{v}$ as a linear combination of other vectors $\mathbf{v}_i$ coincide with our spherical Wachspress coordinates. It is sufficient to consider only vectors $\mathbf{v}_i$ and $\mathbf{v}$ of unit length and to show that the coordinates coincide up to a constant factor c. Then, it follows from Equations (6) and (3), which hold for both sets of coordinates, that they coincide for arbitrary vectors and that $c = 1$.

By Equation (5) and Figure 2, spherical Wachspress coordinates are given by

$$\lambda_i = \frac{1}{\cos\theta_i}\widehat{\lambda}_i \tag{9}$$

where $\widehat{\lambda}_i$ are the planar Wachspress coordinates for the planar polygon with vertices $\widehat{\mathbf{v}}_i$ constructed in Section 2.1. We now show that the same formula holds for the vector coordinates constructed in [JSWD05].

Ju et al.'s vector coordinates are defined for vectors $\mathbf{v}_i$ that are the vertices of a convex spherical polygon. The coordinates are proportional to the area β_i of the triangular faces of the polar dual. The polar dual is the convex polyhedron that is bounded by the planes that have $\mathbf{v}_i$ as normal and pass through the point $\mathbf{v}$ and by the plane perpendicular to $\mathbf{v}$ with distance $\frac{1}{\|\mathbf{v}\|}$ to the point $\mathbf{v}$ (see Figure 3; the polar dual is shown in blue). Let $\bar{\mathbf{v}}$ be the intersection point of $\mathbf{v}$ and the latter plane. Let $\bar{\mathbf{v}}_i$ be the intersection points of the same plane and the rays (green) determined by the $\mathbf{v}_i$. Let $\bar{P}$ be the polygon (shown in red) formed by the $\bar{\mathbf{v}}_i$. Then $\bar{\mathbf{v}}$ and $\bar{P}$ are, by construction, similar to $\mathbf{v}$ and $\widehat{P}$, the polygon defined in Section 2.1. Therefore, the respective Wachspress coordinates coincide: $\widehat{\lambda}_i(\bar{\mathbf{v}};\bar{P}) = \widehat{\lambda}_i(\mathbf{v};\widehat{P})$. Note that the boundary polygon Q (solid blue in Figure 3, left) of the bottom face of the polar dual is dual to $\bar{P}$ (red) with respect to $\bar{\mathbf{v}}$. That is, its edges $\mathbf{a}_i$ are orthogonal to $\bar{\mathbf{v}}_i - \bar{\mathbf{v}}$ (see Appendix A for dual polygons).

The triangle areas β_i can be computed (up to a factor $\frac{1}{2}$) as the product of the length a_i of the edge $\mathbf{a}_i$ and the respective height h_i. The latter can be computed as $h_i = \frac{\|v\|^{-1}}{\cos(\frac{\pi}{2}-\theta_i)} = \frac{\|v\|^{-1}}{\sin\theta_i}$. In the bottom face, the distance r_i of the edge $\mathbf{a}_i$ to the center $\bar{\mathbf{v}}$ is given by $\|v\|^{-1}\tan(\frac{\pi}{2}-\theta_i) = \|v\|^{-1}\cot\theta_i$ and the distance of the intersection points $\bar{\mathbf{v}}_i$ to $\bar{\mathbf{v}}$ is given by $d_i = (1-\|v\|^{-1})\tan\theta_i$. The product $r_i d_i = \frac{\|v\|-1}{\|v\|^2}$ is independent of i. Therefore, Q is (up to scaling) that dual polygon of $\bar{P}$ such that the distance r_i of the edges $\mathbf{a}_i$ to the center $\bar{\mathbf{v}}$ is inverse to the distance d_i between $\bar{\mathbf{v}}_i$ and $\bar{\mathbf{v}}$ (up to a constant factor). The edges of such a polygon have lengths a_i proportional to $d_i\widehat{\lambda}_i$ (see Appendix A). If we put everything together, we obtain the following formula for the vector coordinates

$$\beta_i = \frac{1}{2}a_i h_i = c_1 d_i h_i \widehat{\lambda}_i = c\frac{\widehat{\lambda}_i}{\cos\theta_i}$$

with some constants c and c_1. A comparison with Equation (9) concludes our proof.

3. Barycentric coordinates for closed meshes with polygonal faces

First, we present the approach to compute barycentric coordinates for triangular meshes that was introduced in [JW05]. Then, we show how barycentric coordinates for arbitrary closed polygonal meshes can be obtained by using the spherical barycentric coordinates proposed in Section 2.1. 3D mean value coordinates are computed by Equation (10) if $\mathbf{v}_F$ is calculated by Equation (11) and λ_i by Equation (12).

Let $\mathbf{x} \in \mathbb{R}^3$ be a point. Its barycentric coordinates with respect to a mesh with vertices $\mathbf{v}_i$ consist of coordinate functions $\lambda_i^{3D}(\mathbf{x})$ that fulfill Equations (2) and (3). To define them, we need the following notation: $F(\mathbf{v}_i)$ denotes the set of faces incident to $\mathbf{v}_i$. For a face F, let $V(F)$ denote the set of indices i such that $\mathbf{v}_i$ is incident to F and let $P_F := (\mathbf{v}_i - \mathbf{x})_{i\in V(F)}$ be the boundary polygon of F, relative to $\mathbf{x}$. Using Equation (2), Equation (3) is equivalent to

$$\sum_i \lambda_i^{3D} \cdot (\mathbf{v}_i - \mathbf{x}) = \mathbf{0}. \tag{3′}$$

Thus, it is sufficient to find a solution λ_i^{3D} for Equation (3′). This is done in two steps [JW05]:

- A face vector $\mathbf{v}_F$ is assigned to each face F of the mesh such that $\sum_F \mathbf{v}_F = \mathbf{0}$. (Think of $\mathbf{v}_F$ as some kind of face normal.)
- The face vectors are distributed to their respective face vertices by finding λ_i such that $\sum_{i\in V(F)} \lambda_i \cdot (\mathbf{v}_i - \mathbf{x}) = \mathbf{v}_F$.

While this procedure was proposed only for triangular meshes in [JW05] (in this case, the latter step has a unique solution), we can extend it to arbitrary meshes by employing spherical barycentric coordinates λ_i for the distribution of the face vectors $\mathbf{v}_F$. Using them, we can assign barycentric coordinates to each vertex $\mathbf{v}_i$:

$$\lambda_i^{3D}(\mathbf{x}) := \frac{w_i(\mathbf{x})}{\sum_j w_j(\mathbf{x})}, \quad w_i(\mathbf{x}) := \sum_{F \in F(\mathbf{v}_i)} \lambda_i(\mathbf{v}_F; P_F). \quad (10)$$

Note that P_F is in general not a spherical polygon. Therefore, the λ_i refer to the generalized spherical barycentric coordinates (6). It is clear from the construction that the w_i satisfy Equation (3′). It follows that the λ_i^{3D} satisfy (2) and (3).

We can now vary our 3D barycentric coordinates by the choice of $\mathbf{v}_F$ and the choice of the spherical barycentric coordinates λ_i. In [JW05] is described (for triangular meshes) how $\mathbf{v}_F$ has to be chosen to obtain Wachspress coordinates, mean value coordinates, discrete harmonic coordinates, or any other barycentric coordinates. In the next section, we describe the necessary choices to obtain 3D mean value coordinates for polygonal meshes.

3.1. Mean value coordinates for closed meshes

Mean value coordinates are the most flexible since they can be computed for non-convex meshes with non-convex (planar) faces. The following construction of the associated face vector is due to [FKR05, JSW05]. Let $\mathbf{x}$ be a point inside the body bounded by the mesh. For a face F, let P_F be the boundary polygon with respect to $\mathbf{x}$ as above, and let Q_F be the spherical polygon that is obtained by projecting the vertices of P_F to the unit sphere centered at $\mathbf{x}$. We know from Stokes' theorem that the integral over the unit normals $\mathbf{v}-\mathbf{x}$ of this sphere is zero:

$$\int_{\mathbf{v}-\mathbf{x} \in \mathbb{S}^2} (\mathbf{v}-\mathbf{x}) dS = \mathbf{0}.$$

The Q_F induce a polygonal tessellation of this sphere and we define

$$\mathbf{v}_F := \int_{\mathbf{v}-\mathbf{x} \in Q_F} (\mathbf{v}-\mathbf{x}) dS, \quad \sum_F \mathbf{v}_F = \mathbf{0}.$$

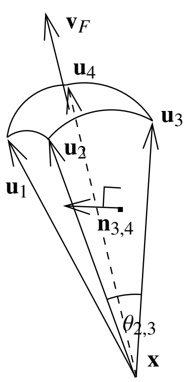

Figure 4: *The face normal* $\mathbf{v}_F$.

Let the vertices of Q_F be $\mathbf{u}_1, \ldots \mathbf{u}_n$. Another application of Stokes' theorem yields the formula

$$\mathbf{v}_F = \sum_{i=1}^{n} \frac{1}{2} \theta_{i,i+1} \mathbf{n}_{i,i+1} \quad (11)$$

where $\theta_{i,i+1}$ is the angle between $\mathbf{u}_i$ and $\mathbf{u}_{i+1}$ and $\mathbf{n}_{i,i+1} := \frac{\mathbf{u}_i \times \mathbf{u}_{i+1}}{\|\mathbf{u}_i \times \mathbf{u}_{i+1}\|}$ is the oriented unit normal to the plane determined by these vectors (Figure 4). To distribute the face vector to the incident vertices, we choose spherical mean value coordinates. This choice of the λ_i leads to 3D mean value coordinates whose restriction to the faces of the mesh yields the planar mean value coordinates of the respective faces (Section 3.2). For each face F, the $\lambda_i(\mathbf{v}_F; P_F)$ can easily be computed with Equations (8) and (6). We obtain

$$\lambda_i = \frac{\|\mathbf{v}_F\|}{\|\mathbf{v}_i - \mathbf{x}\|} \cdot \frac{\tan\frac{\alpha_{i-1}}{2} + \tan\frac{\alpha_i}{2}}{\sin\theta_i} \Big/ \sum_j \cot\theta_j \left(\tan\frac{\alpha_{j-1}}{2} + \tan\frac{\alpha_j}{2}\right). \quad (12)$$

Since the vertices $\mathbf{v}_i$, $i \in V(F)$ of P_F are the boundary vertices of the planar face F, it follows from the construction that the spherical mean value coordinates λ_i are well-defined and positive for convex faces. Consequently, our 3D mean value coordinates are well-defined and positive for points $\mathbf{x}$ in the interior of convex polyhedra. By construction, our mean value coordinates coincide with the mean value coordinates from [FKR05, JSW05] if they are computed for meshes with triangular faces.

3.2. Behavior of the mean value coordinates on the faces

The denominator of Equation (12) becomes zero if $\mathbf{x}$ is contained in a face F of the mesh. In this case, the face vector $\mathbf{v}_F$ is orthogonal to F and Q_F lies on a great circle since its vertices $\frac{\mathbf{v}_i - \mathbf{x}}{\|\mathbf{v}_i - \mathbf{x}\|}$ lie in the plane determined by F. We show now that the 3D mean value coordinates have nevertheless a continuous extension to the faces and that this extension coincides with the 2D mean value coordinates. Assume that $\mathbf{x}$ approaches a point located on the face F. Then $\mathbf{v}_F$ approaches the face normal. It follows that the denominator of the $\lambda_i(\mathbf{v}_F; P_F)$ defined in Equation (12) approaches infinity. Therefore, in the limit (due to the normalization)

$$\lambda_i^{3D}(\mathbf{x}) = \begin{cases} \dfrac{w_i}{\sum_{j \in V(F)} w_j}, \; w_i = \lambda_i(\mathbf{v}_F), & i \in V(F) \\ 0, & \text{otherwise.} \end{cases}$$

This approaches the usual 2D mean value coordinates.

4. Applications

4.1. Interpolation and extrapolation

The most direct application of mean value coordinates is their use for interpolation and extrapolation using Equation (4). In Figure 5, color values are specified on the eight vertices of the cube. In the top row, the values are interpolated on the faces. In the bottom row, the color values are interpolated and extrapolated on a plane that passes through the cube. In the left column, the cube was triangulated before the interpolation. The piecewise linear structure of the interpolation on the triangles is clearly visible. With our 3D mean value coordinates, a triangulation is no longer necessary, and the resulting interpolation is much smoother.

4.2. Space deformations with 3D mean value coordinates

Figure 6 shows an example how mean value coordinates can be used for space deformations. We determine the mean value coordinates of the vertices of the tube with respect to the black control mesh with vertices $\mathbf{v}_i$. Then we deform the

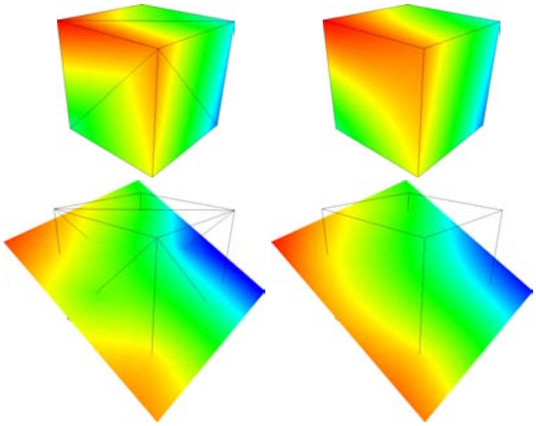

Figure 5: *An example of interpolation of color values using 3D mean value coordinates. The color values are specified at the vertices of the cube. They are interpolated on the faces (top) and on a plane passing through the cube (bottom). If the cube is triangulated beforehand (left), the interpolation is less smooth than with our method (right).*

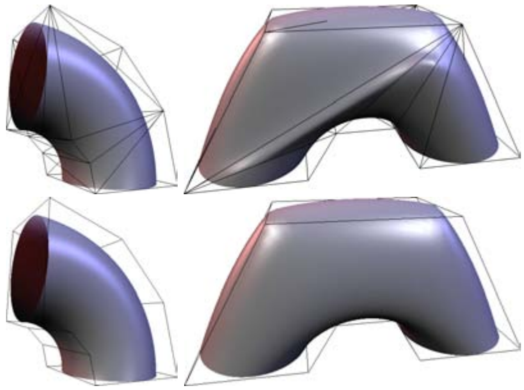

Figure 6: *An example of a space deformation using 3D mean value coordinates with respect to the polygonal control mesh. If the control mesh is triangulated beforehand, strong artifacts may be introduced (top). No triangulation is necessary with our method (bottom).*

control mesh by moving the vertices to points $\mathbf{w}_i$ and calculate the new location of the tube by $\mathbf{x} = \sum_i \lambda_i^{3D}\left(\mathbf{x}; (\mathbf{v}_j)_j\right)\mathbf{w}_i$. Note that we can compute these coordinates for non-convex (control) meshes with non-convex faces (bottom row). If all faces are triangulated, the number of faces is nearly tripled, the result depends on the chosen triangulation, and large artifacts may be introduced (top row).

Although this approach is very simple, it is possible to obtain pleasing results. A more sophisticated framework could use Bernstein polynomials on polyhedra (Section 4.3) to generate free-form deformations [SP86].

Figure 7: *The quadratic mean value Bernstein polynomials B^2_{2000}, B^2_{1100}, and $B^2_{1010} + B^2_{0101}$.*

4.3. Bernstein polynomials on polygons and polyhedra

Bézier surfaces are defined by a linear combination of Bernstein polynomials which are polynomials in barycentric coordinates. Using classical barycentric coordinates, this was only possible for triangles. Using tensor product polynomials, Bernstein polynomials can be defined on quadrangular domains as well, but this leads to a higher degree of the polynomial. The only approaches for general polygons that we are aware of are restricted to convex polygons [LD89, Gol02].

We can define mean value Bernstein polynomials for arbitrary polygons and polyhedra. For a polygon or polyhedron with k vertices, the general form for the Bernstein polynomials in the coordinates $\lambda = (\lambda_1, \ldots \lambda_k)$ is

$$B^n_\alpha(\mathbf{x}) = \frac{n!}{\alpha!}\lambda^\alpha(\mathbf{x})$$

where we use multi-indices $\alpha = (\alpha_1, \ldots \alpha_k) \in \mathbb{N}^k$ with the notation $\alpha! := \alpha_1! \cdots \alpha_k!$ and $\lambda^\alpha := \lambda_1^{\alpha_1} \cdots \lambda_k^{\alpha_k}$. In Figure 7, we show some quadratic Bernstein polynomials on a square using mean value coordinates [Flo03].

Important properties of classical Bézier surfaces like the convex hull property and the de Casteljau algorithm still hold in this extended setup.

4.4. Bézier surfaces on spherical polygonal domains

In the above applications, spherical barycentric coordinates were only indirectly used to construct 3D barycentric coordinates. But they can also be used directly to construct Bézier surfaces on spherical domains. For a triangulation of the sphere, this has been done in [ANS96]. Our extension to arbitrary spherical polygons makes it possible to handle arbitrary tessellations of a sphere. Again, the de Casteljau algorithm can be used for computations of the spherical Bézier patches.

5. Conclusions

We have introduced spherical barycentric coordinates that generalize Ju et al.'s vector coordinates. Our spherical mean value coordinates are defined not only for convex spherical polygons but for arbitrary polygons that are contained in a single hemisphere. We have shown that spherical mean value coordinates can be used to construct 3D mean value coordinates for meshes with arbitrary polygonal faces while so far only 3D mean value coordinates for triangular meshes were known. This concludes the generalization of mean value coordinates from two to three dimensions.

The examples in Section 4 demonstrate that these 3D mean value coordinates are well-defined for arbitrary polyhedra. This is proven for convex polyhedra in this paper. We intend to give a proof for the general case in the near future.

With barycentric coordinates for arbitrary polyhedra in $\mathbb{R}^3$, we can construct spherical barycentric coordinates for the three-dimensional sphere. These can then be used to obtain barycentric coordinates for arbitrary polytopes in $\mathbb{R}^4$ and successively in higher dimensions. It would be interesting to find a general theory for barycentric coordinates for arbitrary polytopes similar to the one given in [FHK06,JW05]. It should shed light on the relationship between "Euclidean" and spherical coordinates. To construct the general 3D mean value coordinates, we used the construction for 3D mean value coordinates for triangular meshes together with the spherical mean value coordinates. However, should we use Wachspress coordinates in both cases to obtain the general Wachspress coordinates? Or should rather the spherical mean value coordinates be used again, due to their better properties? These topics need to be addressed in future work.

Acknowledgements

We are grateful to Tao Ju and Joe Warren for providing us with their manuscripts prior to publication. We would like to thank the anonymous reviewers for their comments and suggestions. The research of the authors has been supported in part by the EU-Project "AIM@SHAPE" FP6 IST Network of Excellence 506766.

References

[ANS96] Alfeld P., Neamtu M., Schumaker L. L.: Bernstein-Bézier polynomials on spheres and sphere-like surfaces. *Comput. Aided Geom. Des. 13*, 4 (1996), 333–349.

[AO06] Arroyo M., Ortiz M.: Local *maximum-entropy* approximation schemes: a seamless bridge between finite elements and meshfree methods. *Int. J. Numer. Meth. Engng 65*, 13 (2006), 2167–2202.

[BF01] Buss S. R., Fillmore J. P.: Spherical averages and applications to spherical splines and interpolation. *ACM Trans. Graph. 20*, 2 (2001), 95–126.

[BW92] Brown J. L., Worsey A. J.: Problems with defining barycentric coordinates for the sphere. *Mathematical Modelling and Numerical Analysis 26* (1992), 37–49.

[DMA02] Desbrun M., Meyer M., Alliez P.: Intrinsic parameterizations of surface meshes. *Computer Graphics Forum 21* (2002), 209–218.

[FHK06] Floater M. S., Hormann K., Kós G.: A general construction of barycentric coordinates over convex polygons. *Adv. Comp. Math. 24*, 1–4 (Jan. 2006), 311–331.

[FKR05] Floater M. S., Kós G., Reimers M.: Mean value coordinates in 3D. *Comp. Aided Geom. Design 22* (2005), 623–631.

[Flo03] Floater M. S.: Mean value coordinates. *Computer Aided Geometric Design 20*, 1 (2003), 19–27.

[Gol02] Goldman R.: *Pyramid Algorithms: A Dynamic Programming Approach to Curves and Surfaces for Geometric Modeling*. Morgan Kaufmann, 2002.

[Gou71] Gouraud H.: Continuous shading of curved surfaces. *IEEE Trans. Computers C-20*, 6 (1971), 623–629.

[HF06] Hormann K., Floater M. S.: Mean value coordinates for arbitrary planar polygons. *ACM Transactions on Graphics* (Mar. 2006). Accepted.

[JSW05] Ju T., Schaefer S., Warren J.: Mean value coordinates for closed triangular meshes. *ACM Trans. Graph. 24*, 3 (2005), 561–566.

[JSWD05] Ju T., Schaefer S., Warren J., Desbrun M.: A geometric construction of coordinates for convex polyhedra using polar duals. In *Proceedings of the Symposium on Geometry Processing* (2005), pp. 181–186.

[JW05] Ju T., Warren J.: *General Constructions of Barycentric Coordinates in a Convex Triangular Polyhedron*. Tech. rep., Washington University in St. Louis, Nov. 2005.

[LD89] Loop C. T., DeRose T. D.: A multisided generalization of Bézier surfaces. *ACM Trans. Graph. 8*, 3 (1989), 204–234.

[LPW*06] Liu Y., Pottmann H., Wallner J., Yang Y.-L., Wang W.: Geometric modeling with conical meshes and developable surfaces. *ACM Transactions on Graphics, Proceedings of SIGGRAPH 2006* (2006). To appear.

[MBLD02] Meyer M., Barr A., Lee H., Desbrun M.: Generalized barycentric coordinates on irregular polygons. *J. Graph. Tools 7*, 1 (2002), 13–22.

[Möb27] Möbius A. F.: *Der barycentrische Calcul*. Johann Ambrosius Barth, Leipzig, 1827.

[Möb46] Möbius A. F.: Ueber eine neue Behandlungsweise der analytischen Sphärik. In *Abhandlungen bei Begründung der Königl. Sächs. Gesellschaft der Wissenschaften*. Jablonowski Gesellschaft, 1846, pp. 45–86.

[Pho75] Phong B. T.: Illumination for computer generated pictures. *Communications of ACM 18*, 6 (1975), 311–317.

[PP93] Pinkall U., Polthier K.: Computing discrete minimal surfaces and their conjugates. *Experimental Mathematics 2*, 1 (1993), 15–36.

[SAPH04] Schreiner J., Asirvatham A., Praun E., Hoppe H.: Inter-surface mapping. *ACM Trans. Graph. 23*, 3 (2004), 870–877.

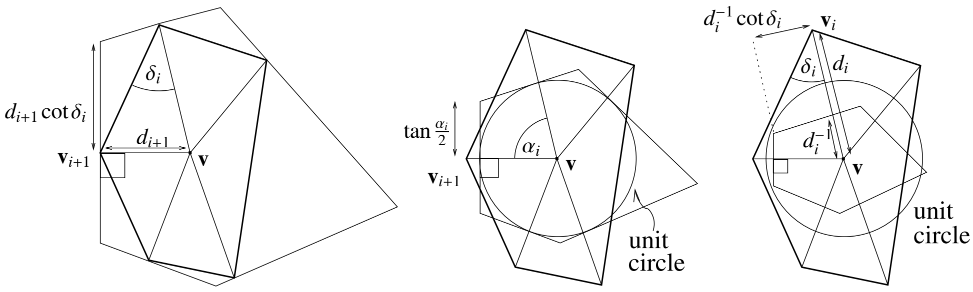

Figure 8: *A geometric construction of the discrete harmonic, mean value, and Wachspress coordinates (from left to right).*

[Sib80] Sibson R.: A vector identity for the Dirichlet tessellation. *Math. Proc. Cambridge Phil. Soc. 87* (1980).

[SJW06] Schaefer S., Ju T., Warren J.: A unified, integral construction for coordinates over closed curves. *Computer Aided Geometric Design* (2006). Submitted.

[SM06] Sukumar N., Malsch E. A.: Recent advances in the construction of polygonal interpolants. *Arch. Comput. Meth. Engng. 13*, 1 (2006), 129–163.

[SP86] Sederberg T. W., Parry S. R.: Free-form deformation of solid geometric models. In *Computer Graphics, Proceedings of ACM SIGGRAPH* (1986), pp. 151–160.

[Wac75] Wachspress E. L.: *A Rational Finite Element Basis*, vol. 114. Academic Press, New York, 1975.

[War96] Warren J.: Barycentric coordinates for convex polytopes. *Adv. Comp. Math. 6*, 2 (1996), 97–108.

Appendix A: A geometric interpretation for planar barycentric coordinates

Here, we present a unified, geometric, and intuitive construction that explains the "linear precision" property of an especially interesting one-parameter family of barycentric coordinates that was introduced in [FHK06]. A different, but equivalent, approach was recently presented in [SJW06]. With this construction, we can derive analogues of the discrete harmonic, mean value, and Wachspress coordinates for arbitrary dimensions. In this paper, we used it in Section 2.3 to show that our spherical Wachspress coordinates and Ju et al.'s vector coordinates coincide. Nevertheless, this construction constitutes an independent contribution on its own.

Our construction is indicated in Figure 8. It is based on a theorem of Minkowski which states that the sum over the edge normals of a polygon, weighted with the respective edge lengths, is zero. Consider a polygon with vertices $\mathbf{v}_i$. It is always possible to construct a dual polygon (that may have self-intersections) with respect to a vertex $\mathbf{v}$ whose edges are orthogonal to the edges $\mathbf{v}\mathbf{v}_i$ and whose vertices are given by the intersection point of two consecutive edges. In fact, there are even infinitely many dual polygons since we can choose the intersection point of the dual edges with the line given by $\mathbf{v}\mathbf{v}_i$ freely. Since the normals of the dual edges are given by the edges $\mathbf{v}\mathbf{v}_i$, the lengths a_i of the dual edges yield homogeneous coordinates w_i for $\mathbf{v}$ that satisfy property (3′). Since the edges $\mathbf{v}\mathbf{v}_i$ don't have unit length in general, the exact relationship between a_i and $\widehat{\lambda}_i = \frac{w_i}{\sum_j w_j}$ is $a_i = d_i w_i$ where $d_i = \|\mathbf{v}\mathbf{v}_i\|$. Negative weights correspond to inversely oriented dual edges.

In Figure 8, three particular choices for the intersection point of the dual edges are depicted. On the left, the dual edges pass through the points $\mathbf{v}_i$, in the middle, the dual edges have constant distance to $\mathbf{v}$, and on the right, the distance of the dual edges to $\mathbf{v}$ is d_i^{-1}. Using a little trigonometry, it is easy to show that these choices correspond to the standard formulae for discrete harmonic, mean value, and Wachspress coordinates [PP93, Flo03, MBLD02]. In fact, this construction had been used to derive the discrete harmonic coordinates.

Now, it is natural to ask what kind of coordinates are obtained if the distance of the dual edges to $\mathbf{v}$ is chosen as d_i^p, $p \in \mathbb{R}$. The answer, given as a formula, is

$$w_{i,p} = \frac{1}{d_i}\left(\frac{d_{i+1}^p - d_i^p\cos\alpha_i}{\sin\alpha_i} + \frac{d_{i-1}^p - d_i^p\cos\alpha_{i-1}}{\sin\alpha_{i-1}}\right).$$

If we compare this to the one-parameter family of barycentric coordinates $\widehat{w}_{i,p}$ from [FHK06], we see that $w_{i,p} = \frac{1}{2}\widehat{w}_{i,p+1}$. Therefore, both families generate the same barycentric coordinates (after normalization), and the analysis of Floater et al. applies to our family as well:

Corollary A.1 ([FHK06]) The only members of the one-parameter family $w_{i,p}$ which are positive for all convex polygons are the Wachspress and the mean value coordinates.

Another appealing property of this geometric construction is that it easily generalizes to higher dimensions, and barycentric coordinates for polytopes with simplicial boundary can be derived. In the three-dimensional case, the analogous weights $w_{i,p}$ lead to three-dimensional Wachspress coordinates for $p = -1$, but for $p = 0$ and $p = 1$, they do not correspond to the mean value and discrete harmonic coordinates constructed in [JW05] unlike in the two-dimensional case.